Greek Letters

$\xi(x)$ = instantaneous mean of crystal growth rate
$\sigma^2(x)$ = instantaneous variance of crystal growth rate

LITERATURE CITED

Cox, D. R., and H. D. Miller, *The Theory of Stochastic Processes*, John Wiley,New York (1965).

Fan, L. T., J. R. Too and R. Nassar, "Stochastic Flow Reactor Modeling: A General Continuous Time Compartmental Model With First-Order Reactions," *Residence Time Distribution Theory In Chemical Engineering*, edited by Pethö and R. D. Noble, Verlag Chemie Gmbh., D-6940, Weinheim (1982).

Froment, G. F., and K. B. Bischoff, *Chemical Reactor Analysis and Design*, John Wiley, New York (1979).

Garside, J., I. T. Rusli, and M. A. Larson, "Origin and Size Distribution of Secondary Nuclei," *AIChE J.*, **25**, 57 (1979).

Hartel, R. W., et al., "Crystal Kinetics for Sucrose-Water System," *AIChE Sym. Ser.*, **76**, (193), 65 (1980).

Hulburt, H. M., and S. Katz, "Some Problems in Particle Technology," *Chem. Eng. Sci.*, **19**, 555 (1964).

Jančić, S., and J. Garside, "On the Determination of Crystallization Kinetics from Crystal Size Distribution Data," *Chem. Eng. Sci.*, **30**, 1299 (1975).

Lieb, E. B., "Perfect-Mixing Approximation of Imperfectly Mixed Continuous Crystallizers," *AIChE J.*, **19**, 646 (1973).

Melikhov, I. V., and L. B. Berliner, "Simulation of Batch Crystallization," *Chem. Eng. Sci.*, **36**, 1021 (1981).

Ramkrishna, D., and J. D. Borwanker, "A Puristic Analysis of Population Balance-I," *Chem. Eng. Sci.*, **28**, 1423 (1973).

Randolph, A. D., "A Perspective on Population Models for Crystal-size Distribution," 7th Symp. of Ind. Crystalliz., Warsaw, Poland (Sept. 25–27, 1978).

Randolph, A. D., and M. A. Larson, "Transient and Steady State Size Distributions in Continuous Mixed Suspension Crystallizers," *AIChE J.*, **8**, 639 (1962).

Randolph, A. D., and M. A. Larson, *Theory of Particulate Processes*, Academic Press, New York (1971).

Randolph, A. D., and E. T. White, "Modeling Size Dispersion in Prediction of Crystal-size Distribution," *Chem Eng. Sci.*, **32**, 1067 (1977).

Sherwin, M. B., R. Shinnar, and S. Katz, "Dynamic Behavior of the Well-Mixed Isothermal Crystallizer," *AIChE J.*, **13**, 1141 (1967).

Sommerfeld, A., *Partial Differential Equations in Physics*, Academic Press, New York (1949).

Manuscript received November 18, 1982; revision received August 2, and accepted August 24, 1983.

Collocation Solution of Creeping Newtonian Flow through Sinusoidal Tubes: a Correction

J. N. TILTON and A. C. PAYATAKES

Chemical Engineering Department
University of Houston
Houston, TX 77004

Periodically constricted tubes have frequently been used in modeling flow through porous media (Payatakes et al., 1973a,b,c; 1974a,b; Slattery, 1974; Sheffield and Metzner, 1976; Payatakes and Neira, 1977; Fedkiw and Newman, 1977; Neira and Payatakes, 1978, 1979; Deiber and Schowalter, 1979, 1981; Oh and Slattery, 1979; Tien and Payatakes, 1979; Payatakes et al., 1980; Giordano and Slattery, 1982). Laminar flow through tubes with variable radius has also been studied in connection with other applications (Dodson et al., 1971; Chow and Soda, 1972, 1973a,b; Lessen and Huang, 1976).

Payatakes et al. (1973b) used a finite difference method to solve the full Navier-Stokes equations for flow through a periodically constricted tube. Thus, their solution remains valid when the nonlinear inertial terms become important (which is the case for Reynolds number greater than roughly 1 to 30). In many cases of practical interest, including oil flow through porous reservoir rock, inertial effects may be neglected. Neira and Payatakes (1979) used a collocation method to solve Stokes' equation for creeping flow in a sinusoidal tube. A desirable feature of the collocation method is the analytical form of the approximate solution. Unlike the finite difference method, no interpolation is required to compute quantities at off-node positions, and the collocation solution is well suited to analytical manipulation.

Regrettably, the collocation solution of Neira and Payatakes (1979) is unsatisfactory because it gives a velocity singularity along the tube axis. This paper presents a modification of their solution that rectifies this problem.

Figure 1 depicts a segment of a tube with wall radius varying sinusoidally with axial position. The tube has minimum radius r_1, maximum radius r_2, and wavelength h. Mean radii and reduced amplitudes are defined by $r_a = (r_1 + r_2)/2$ and $b = (r_2 - r_1)/(r_2 + r_1)$, respectively. It is convenient to introduce dimensionless variables as follows:

$$r^* = r/h,\ r_1^* = r_1/h,\ r_2^* = r_2/h,\ r_a^* = r_a/h,\ z^* = z/h,\ r_w^* = r_w/h \tag{1}$$

The dimensionless wall radius is given by:

$$r_w^* = r_a^*[1 + b\sin 2\pi(z^* - 1/4)] \tag{2}$$

The tube constriction or point of minimum radius occurs at the origin of the z-axis. The average velocity at this cross section is denoted by v_o. This velocity is used to form dimensionless velocity components:

$$v_r^* = \frac{v_r}{v_o}, \quad v_z^* = \frac{v_z}{v_o} \tag{3}$$

A dimensionless stream function is defined as follows:

$$v_r^* = \frac{1}{r^*}\frac{\partial \psi^*}{\partial z^*}, \quad v_z^* = -\frac{1}{r^*}\frac{\partial \psi^*}{\partial r^*} \tag{4}$$

Stokes' equation for creeping flow may be expressed in terms of the stream function as

$$E^{*4}\psi^* = 0 \tag{5}$$

where

$$E^{*2} \equiv \frac{\partial^2}{\partial r^{*2}} - \frac{1}{r^*}\frac{\partial}{\partial r^*} + \frac{\partial^2}{\partial z^{*2}} \tag{6}$$

Equation 5 must be solved subject to the following boundary conditions:

1. No slip at the tube wall.

$$\frac{\partial \psi^*}{\partial r^*} = \frac{\partial \psi^*}{\partial z^*} = 0 \text{ at } r^* = r_w^*(z^*) \tag{7}$$

Equation 7 requires ψ^* = constant along the wall. For conve-

Correspondence concerning this paper should be directed to J. N. Tilton.
A. C. Payatakes is also at the Department of Chemical Engineering, Polytechnic School, University of Patras, Patras, Greece.

TABLE 1. VALUES OF C_k FOR VARIOUS TUBE GEOMETRIES; $n_r = n_z = \sqrt{N}$ IN ALL CASES

k \ r_1^*/r_2^*	0.2	0.4	0.6	0.8
		$r_2^* = 0.05$		
1	-7.7866×10^{-7}	-1.7637×10^{-6}	-1.7723×10^{-6}	-7.9015×10^{-7}
2	-1.1942×10^{-8}	-1.3276×10^{-8}	-2.9048×10^{-9}	1.7811×10^{-9}
3	-1.6586×10^{-10}	-5.8593×10^{-11}	2.4838×10^{-11}	3.6887×10^{-12}
4	3.9203×10^{-7}	1.3759×10^{-6}	2.3632×10^{-6}	2.3657×10^{-6}
5	1.0072×10^{-8}	1.8811×10^{-8}	1.1363×10^{-8}	-1.8847×10^{-9}
6	1.2893×10^{-10}	8.0510×10^{-11}	-4.0902×10^{-11}	-2.2990×10^{-11}
7	5.0932×10^{-7}	1.1609×10^{-6}	1.1713×10^{-6}	5.2320×10^{-7}
8	8.5684×10^{-9}	2.8298×10^{-9}	-1.0891×10^{-8}	-9.5850×10^{-9}
9	1.9328×10^{-10}	9.3375×10^{-11}	3.9900×10^{-11}	5.3247×10^{-11}
		$r_2^* = 0.10$		
1	-1.1970×10^{-5}	-2.7627×10^{-5}	-2.8158×10^{-5}	-1.2669×10^{-5}
2	-6.9577×10^{-7}	-8.0652×10^{-7}	-1.8267×10^{-7}	1.1309×10^{-7}
3	-3.8109×10^{-8}	-1.3597×10^{-8}	6.2137×10^{-9}	9.0370×10^{-10}
4	6.1461×10^{-6}	2.1739×10^{-5}	3.7548×10^{-5}	3.7709×10^{-5}
5	5.9969×10^{-7}	1.1502×10^{-6}	7.0725×10^{-7}	-1.2121×10^{-7}
6	3.0460×10^{-8}	1.9193×10^{-8}	-1.0175×10^{-8}	-5.6421×10^{-9}
7	7.3960×10^{-6}	1.7503×10^{-5}	1.8139×10^{-5}	8.2270×10^{-6}
8	4.6016×10^{-7}	1.3355×10^{-7}	6.8396×10^{-7}	-5.9957×10^{-7}
9	4.2854×10^{-8}	2.1211×10^{-8}	9.6750×10^{-9}	1.3091×10^{-8}
		$r_2^* = 0.20$		
1	-1.6624×10^{-4}	-4.0894×10^{-4}	-4.3850×10^{-4}	-2.0426×10^{-4}
2	-3.2359×10^{-5}	-4.2826×10^{-5}	-1.0996×10^{-5}	7.0059×10^{-6}
3	-5.7343×10^{-6}	-2.4158×10^{-6}	1.4426×10^{-6}	1.9605×10^{-7}
4	-1.0148×10^{-6}	3.3105×10^{-4}	5.8402×10^{-4}	5.9393×10^{-4}
5	9.1751×10^{-5}	6.2016×10^{-5}	4.0688×10^{-5}	-7.8101×10^{-6}
6	2.7097×10^{-5}	3.7708×10^{-6}	-2.3156×10^{-6}	-1.2307×10^{-6}
7	6.2983×10^{-6}	2.2392×10^{-4}	2.5718×10^{-4}	1.2431×10^{-4}
8	1.2893×10^{-6}	2.8491×10^{-7}	-4.0398×10^{-5}	-3.5265×10^{-5}
9	8.6631×10^{-5}	3.3849×10^{-6}	2.0177×10^{-6}	2.8470×10^{-6}
10	1.9456×10^{-5}			
11	1.5425×10^{-6}			
12	1.5577×10^{-7}			
13	1.3361×10^{-5}			
14	-1.0801×10^{-5}			
15	-2.3158×10^{-6}			
16	-9.2707×10^{-7}			
		$r_2^* = 0.50$		
1	-3.3319×10^{-3}	-1.0297×10^{-2}	-1.4105×10^{-2}	-8.0709×10^{-3}
2	-1.9982×10^{-3}	-4.2557×10^{-3}	-1.9624×10^{-3}	1.2625×10^{-3}
3	-1.1603×10^{-3}	-1.0803×10^{-3}	3.7121×10^{-4}	1.5718×10^{-4}
4	-5.4852×10^{-4}	-8.5968×10^{-4}	3.7202×10^{-4}	2.0313×10^{-2}
5	-1.3090×10^{-4}	5.1909×10^{-4}	1.8021×10^{-2}	-1.3415×10^{-3}
6	-3.9396×10^{-4}	8.8185×10^{-3}	5.1377×10^{-3}	-8.7954×10^{-4}
7	2.0444×10^{-3}	5.5151×10^{-3}	5.4026×10^{-4}	4.5891×10^{-3}
8	1.7273×10^{-3}	1.7620×10^{-3}	-1.0790×10^{-3}	-5.9911×10^{-3}
9	1.2594×10^{-3}	1.9362×10^{-3}	6.7731×10^{-3}	1.9999×10^{-3}
10	6.2313×10^{-4}	-8.2058×10^{-4}	-2.9028×10^{-3}	
11	-3.0513×10^{-5}	4.0067×10^{-3}	-3.0582×10^{-3}	
12	7.3060×10^{-4}	4.4157×10^{-4}	1.2332×10^{-3}	
13	9.7707×10^{-4}	3.7874×10^{-4}	2.4548×10^{-3}	
14	6.5179×10^{-4}	-2.1513×10^{-3}	-5.3291×10^{-3}	
15	1.4738×10^{-4}	3.5312×10^{-4}	3.6536×10^{-3}	
16	1.8869×10^{-4}	2.1026×10^{-3}	-8.7350×10^{-4}	
17	4.2930×10^{-4}	-1.0078×10^{-3}		
18	-4.4073×10^{-4}	-2.3343×10^{-3}		
19	6.6479×10^{-4}	1.0589×10^{-3}		
20	3.2300×10^{-5}	7.7460×10^{-5}		
21	8.6306×10^{-5}	9.0095×10^{-4}		
22	-4.4260×10^{-4}	-2.2277×10^{-3}		
23	-2.8776×10^{-4}	1.6183×10^{-3}		
24	-6.9596×10^{-6}	-3.3273×10^{-4}		
25	3.3305×10^{-4}	2.9421×10^{-5}		
26	-6.1528×10^{-5}			
27	-5.2856×10^{-4}			
28	1.7567×10^{-4}			
29	-1.2174×10^{-4}			
30	2.0466×10^{-4}			
31	1.6961×10^{-4}			
32	-3.5637×10^{-4}			
33	1.7389×10^{-4}			
34	-3.1082×10^{-5}			
35	1.0702×10^{-4}			
36	-6.3611×10^{-5}			

TABLE I *Continued*

r_1^*/r_2^* k	0.2	0.4	0.6	0.8
		$r_2^* = 1.00$		
1		-5.9539×10^{-2}	-1.1335×10^{-1}	-1.0715×10^{-1}
2		-4.8388×10^{-2}	-6.0115×10^{-2}	2.6071×10^{-2}
3		-5.3348×10^{-2}	-1.3790×10^{-2}	2.5470×10^{-2}
4		5.8610×10^{-2}	2.3035×10^{-2}	-1.1800×10^{-2}
5		-1.4745×10^{-1}	3.4806×10^{-2}	2.0101×10^{-1}
6		8.5160×10^{-2}	-1.9432×10^{-2}	-1.1961×10^{-2}
7		4.0323×10^{-2}	1.1853×10^{-1}	-6.5444×10^{-2}
8		4.4998×10^{-2}	1.0459×10^{-1}	1.8602×10^{-2}
9		1.1640×10^{-1}	7.3543×10^{-2}	7.1524×10^{-2}
10		-1.6910×10^{-1}	-5.9086×10^{-2}	-1.3093×10^{-1}
11		-3.3167×10^{-1}	-4.7965×10^{-2}	3.6016×10^{-2}
12		-1.6724×10^{-1}	2.3180×10^{-2}	2.1154×10^{-2}
13		2.9990×10^{-2}	7.0029×10^{-2}	3.1947×10^{-2}
14		1.7119×10^{-2}	-2.1765×10^{-2}	-1.4755×10^{-1}
15		-5.4441×10^{-2}	-7.2066×10^{-2}	2.1426×10^{-1}
16		1.9261×10^{-1}	-2.9560×10^{-2}	-9.9256×10^{-2}
17		-3.1550×10^{-1}	3.8618×10^{-2}	
18		1.2680×10^{-1}	7.6328×10^{-3}	
19		2.0256×10^{-2}	4.1281×10^{-2}	
20		-1.9168×10^{-2}	-8.4984×10^{-2}	
21		7.5728×10^{-2}	3.9247×10^{-2}	
22		-2.5224×10^{-1}	-9.7146×10^{-2}	
23		-2.3777×10^{-1}	2.0651×10^{-1}	
24		-6.3923×10^{-2}	-1.0539×10^{-1}	
25		1.3384×10^{-2}	2.2893×10^{-2}	
26		-1.0189×10^{-2}	-7.8318×10^{-2}	
27		-7.8772×10^{-2}	-5.4983×10^{-3}	
28		1.4291×10^{-1}	2.8106×10^{-1}	
29		-7.9285×10^{-2}	-3.4990×10^{-1}	
30		1.1863×10^{-2}	1.2980×10^{-1}	
31		8.0134×10^{-3}	1.1907×10^{-2}	
32		-4.2536×10^{-2}	-1.0129×10^{-1}	
33		8.4238×10^{-2}	3.2208×10^{-1}	
34		-8.0833×10^{-2}	-4.9027×10^{-1}	
35		3.9118×10^{-2}	3.6131×10^{-1}	
36		-8.0071×10^{-3}	-1.0375×10^{-1}	

nience, $\psi^* = 0$ is chosen. Then, an integral mass balance over a cross-section of the tube gives

$$\psi^*(0,z^*) = \frac{r_1^{*2}}{2}. \tag{8}$$

2. For an axisymmetric flow the radial velocity and radial derivative of the axial velocity vanish at the centerline:

$$\frac{1}{r^*}\frac{\partial\psi^*}{\partial z^*} = \frac{\partial}{\partial r^*}\left(\frac{1}{r^*}\frac{\partial\psi^*}{\partial r^*}\right) = 0 \text{ at } r^* = 0 \tag{9}$$

The second of these conditions is not satisfied by the original solution of Neira and Payatakes (1979).

3. Periodicity of the fully developed flow requires that for any integer i,

$$\psi^*(r^*,z^*) = \psi^*(r^*,z^*+i). \tag{10}$$

4. The symmetry of creeping flow around $z^* = 0$ requires that

$$\psi^*(r^*,z^*) = \psi^*(r^*,-z^*). \tag{11}$$

Neira and Payatakes (1979) transformed the sinusoidal domain into a rectangular one by defining a new radial coordinate:

$$\xi = \frac{r^*}{r_w^*(z^*)} \tag{12}$$

They obtained a collocation solution of the form

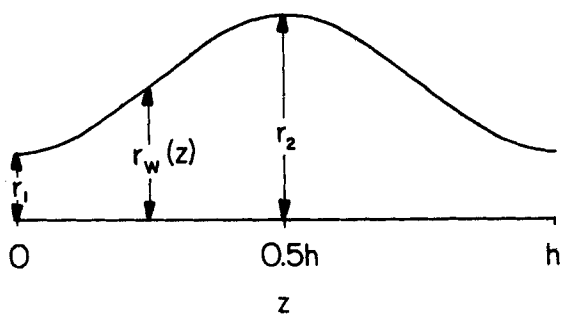

Figure 1. Sinusoidal tube geometry.

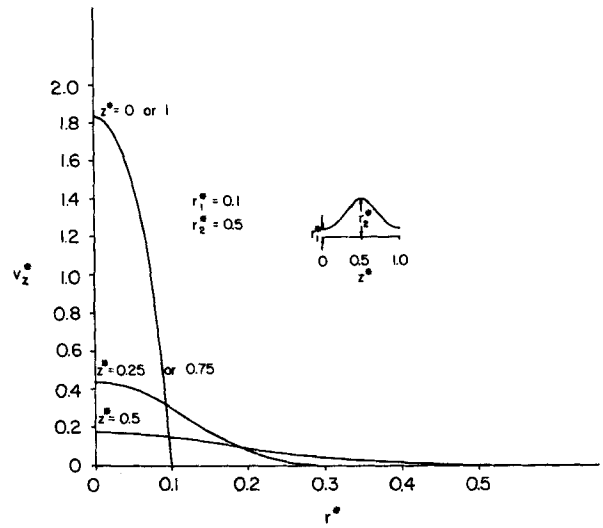

Figure 2. Dimensionless axial velocity profiles for a representative tube geometry.

TABLE 2. DIMENSIONLESS PRESSURE DROP ΔP_1^* IN ONE TUBE SEGMENT AT $N_{Re} = 1$ (NEGLECTING INERTIA)

r_1^*/r_2^*	r_2^* = 0.05	0.06	0.07	0.08	0.09	0.10
0.1	33,830	23,510	17,290	13,260	10,490	8,511
0.2	12,920	8,989	6,616	5,076	4,020	3,265
0.3	7,705	5,360	3,946	3,028	2,399	1,949
0.4	5,555	3,864	2,844	2,183	1,729	1,404
0.5	4,469	3,108	2,287	1,754	1,389	1,128
0.6	3,864	2,686	1,976	1,515	1,199	972.6
0.7	3,517	2,444	1,797	1,377	1,089	882.9
0.8	3,323	2,308	1,696	1,299	1,027	832.3
0.9	3,227	2,241	1,647	1,261	996.4	807.2
1.0	3,200	2,222	1,633	1,250	987.7	800.0
	0.12	0.14	0.16	0.18	0.20	0.23
0.1	5,933	4,378	3,368	2,676	2,181	1,666
0.2	2,280	1,687	1,302	1,037	848.1	651.2
0.3	1,362	1,009	779.1	621.6	508.9	391.5
0.4	981.4	726.4	560.8	447.3	366.0	281.4
0.5	787.2	581.9	448.7	357.3	291.9	223.9
0.6	678.0	500.4	385.1	306.0	249.4	190.6
0.7	614.5	452.8	347.7	275.7	224.2	170.7
0.8	578.6	425.6	326.4	258.3	209.6	159.0
0.9	560.7	412.1	315.6	249.5	202.2	153.0
1.0	555.6	408.2	312.5	246.9	200.0	151.2
	0.26	0.30	0.35	0.40	0.45	0.50
0.1	1,318	1,006	755.9	592.9	480.6	400.0
0.2	518.2	398.8	302.7	239.9	196.4	165.0
0.3	312.2	240.9	183.5	146.0	119.9	101.1
0.4	224.2	172.9	131.6	104.5	85.78	72.18
0.5	177.9	136.7	103.5	81.85	66.85	55.99
0.6	150.9	115.3	86.68	68.03	55.17	45.88
0.7	134.5	102.1	76.17	59.27	47.64	39.28
0.8	124.9	94.27	69.76	53.84	42.91	35.08
0.9	119.8	90.14	66.35	50.91	40.32	32.74
1.0	118.3	88.89	65.31	50.00	39.51	32.00
	0.6	0.7	0.8	0.9	1.0	
0.1	294.0	229	187	158	140	
0.2	123.4	97.63	80.41	68.3	59.4	
0.3	75.88	60.12	49.46	41.84	36.2	
0.4	54.00	42.58	34.81	29.21	25.01	
0.5	41.52	32.45	26.28	21.85	18.52	
0.6	33.58	25.93	20.77	17.10	14.36	
0.7	28.28	21.52	17.03	13.86	11.54	
0.8	24.82	18.59	14.50	11.67	9.610	
0.9	22.85	16.88	13.00	10.33	8.414	
1.0	22.22	16.33	12.50	9.876	8.000	

$$\psi^* = \frac{1}{2} r_1^{*2} (1 - \xi)^2 + \sum_{k=1}^{N} C_k \xi (1 - \xi)^{i+1} \cos 2\pi (j - 1) z^* \quad (13)$$

with

$$i = 1,\ldots,n_r \qquad j = 1,\ldots,n_z$$
$$k = (j - 1)n_r + i \qquad N = n_r n_z \quad (14)$$

where n_r and n_z are the numbers of collocation points in the r and z directions, respectively, and N is the total number of interior collocation points. If this stream function solution, with the coordinate transformation expressed by Eq. 12, is used to compute axial velocities, a singularity is obtained at $r^* = 0$, and boundary condition 2 is violated. All the boundary conditions, including 2, are satisfied if Eq. 12 is replaced by

$$\xi = \left(\frac{r^*}{r_w^*(z^*)} \right)^2 . \quad (15)$$

It may be noted that with ξ defined by Eq. 15, the first term in Eq. 14 is the Hagen-Poiseuille solution for a cylindrical tube. The remaining N terms are corrections to the basic Hagen-Poiseuille flow accounting for the sinusoidal shape.

The collocation points in the z direction are chosen as the zeroes of the first omitted cosine function of the trial expansion (Mehler quadrature points).

$$z_j^* = (j - 0.5)/(2n_z), \qquad j = 1,\ldots,n_z \quad (16)$$

In the ξ direction, the points are chosen as the roots of the nth degree Jacobi polynomials $P_{n_r}^{(0,0)}(\xi)$. This choice of collocation points was successfully employed by Neira and Payatakes (1978) to solve Stokes' equation for flow through periodically constricted tubes with wall cusps.

The expansion coefficients C_k are determined by requiring the residuals of Stokes' equation to vanish at the collocation points. The resulting system of N linear algebraic equations in N unknowns is solved by Gaussian elimination.

Table 1 gives the collocation coefficients for several tube geometries. The larger numbers of collocation coefficients for tubes with small values of r_1^*/r_2^* and/or large values of r_2^* reflect the greater numbers of collocation points needed to achieve convergence. In many cases excellent convergence is obtained using only 9 or 16 collocation points.

The velocity components may be computed from the collocation solution using

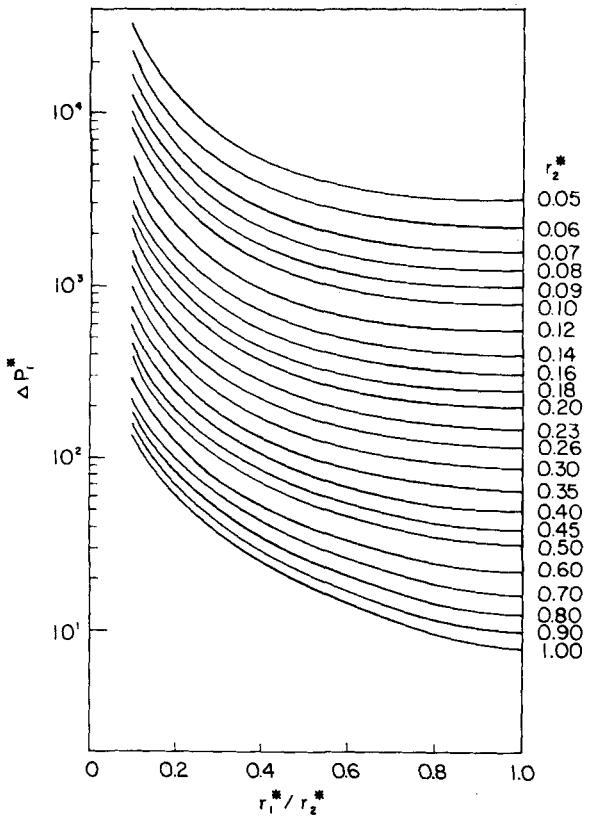

Figure 3. Dimensionless pressure drop along one tube segment for various geometries.

$$v_r^* = \frac{1}{r^*}\left[\left(\frac{\partial \xi}{\partial z^*}\right)_{r^*}\left(\frac{\partial \psi^*}{\partial \xi}\right)_{z^*} + \left(\frac{\partial \psi^*}{\partial z^*}\right)_{\xi}\right] \tag{17}$$

$$v_z^* = -\frac{1}{r^*}\left(\frac{\partial \xi}{\partial r^*}\right)_{z^*}\left(\frac{\partial \psi^*}{\partial \xi}\right)_{z^*} \tag{18}$$

Axial velocity profiles for a sample tube geometry are illustrated in Figure 2.

Following Neira and Payatakes (1978, 1979), a dimensionless pressure drop is defined by

$$\Delta P^* = \frac{\Delta P}{\rho v_o^2} \tag{19}$$

where ΔP is the pressure drop along one tube wavelength.

$$\Delta P^* = \frac{\Delta P_1^*}{N_{Re}}; \qquad N_{Re} = \frac{h v_o}{\nu} \tag{20}$$

where ΔP_1^* is the dimensionless pressure drop at $N_{Re} = 1$, neglecting inertial effects (alternatively, the pressure drop could be rendered dimensionless using the characteristic viscous stress, in which case no Reynolds number correction would be needed). Values of ΔP_1^* calculated by volume integration of the viscous dissipation function (Bird et al., 1960) are presented in graphical form in Figure 3. (* Under creeping flow conditions, the pressure at cross sections of minimum and maximum radius is independent of radial position.) The results are also given in tabular form, suitable for numerical interpolation, in Table 2. Pressure drops were also computed by line integration of the equation of motion, with excellent agreement obtained. The values of ΔP_1^* calculated here agree quite closely with those originally reported by Neira and Payatakes (1979). Evidently, the velocity singularity in the original solution causes overestimation of the dissipation in a small enough volume that the calculation of the pressure drop is not significantly affected.

* Under creeping flow conditions

ACKNOWLEDGMENT

We would like to express our appreciation to Ulli Nollert of Cornell University for his advice.

NOTATION

$b = \dfrac{r_2 - r_1}{r_2 + r_1}$ = reduced amplitude

C_k = collocation expansion coefficients

h = wavelength

$N = n_r n_z$ = number of interior collocation points

$N_{Re} = \dfrac{h v_o}{\nu}$ = Reynolds number

n_r, n_z = number of radial and axial expansion functions (or collocation points), respectively

r, r^* = radial and dimensionless radial coordinates, respectively

$r_a = \dfrac{r_1 + r_2}{2}$ = arithmetic mean radius

r_a^* = dimensionless arithmetic mean radius

$r_w(z)$ = wall radius

$r_w^*(z^*)$ = dimensionless wall radius

r_1, r_2 = minimum and maximum radii, respectively

r_1^*, r_2^* = dimensionless minimum and maximum radii, respectively

v_r, v_z = radial and axial velocity components, respectively

v_r^*, v_z^* = dimensionless radial and axial velocity components, respectively

v_o = mean velocity at a cross section of minimum radius

z, z^* = axial and dimensionless axial coordinates, respectively

Greek Letters

$\Delta P, \Delta P^*$ = pressure drop and dimensionless pressure drop along one tube segment, respectively

ΔP_1^* = value of ΔP^* for $N_{Re} = 1$ (under the assumption of creeping flow)

ν = kinematic viscosity

ξ = new radial coordinate

ψ^* = dimensionless stream function

LITERATURE CITED

Bird, R. B., W. E. Stewart, and E. N. Lightfoot, *Transport Phenomena*, John Wiley, New York (1960).

Chow, J. C. F., and K. Soda, "Laminar Flow in Tubes with Constriction," *Phys. Fluids*, **15**, 1700 (1972).

Chow, J. C. F., and K. Soda, "Heat or Mass Transfer in Laminar Flow in Conduits with Constriction," *J. Heat Transfer*, **95**, 352 (1973a).

Chow, J. C. F., and K. Soda, "Laminar Flow and Blood Oxygenation in Channels with Boundary Irregularities," *J. Applied Mechanics*, **40**, 843 (1973b).

Deiber, J. A., and W. R. Schowalter, "Flow Through Tubes with Sinusoidal Axial Variations in Diameter," *AIChE J.*, **25**, 638 (1979).

Deiber, J. A., and W. R. Schowalter, "Modeling the Flow of Viscoelastic Fluids Through Porous Media," *AIChE J.*, **27**, 912 (1981).

Dodson, A. G., P. Townsend, and K. Walters, "On the Flow of Newtonian and non-Newtonian Liquids Through Corrugated Pipes," *Rheol. Acta*, **10**, 508 (1971).

Fedkiw, P., and J. Newman, "Simulation of a Packed Bed as an Array of Periodically Constricted Tubes I. Creeping Flow," *AIChE J.*, **23**, 255 (1977).

Giordano, R. M., and J. C. Slattery, "Interfacial Effects Upon Displacement in Sinusoidal Capillaries," *AIChE Symp. Ser.*, **78**, 58 (1982).
Lessen, M., and P.-S. Huang, "Poiseuille Flow in a Pipe with Axially Symmetric Wavy Walls," *Phys. Fluids*, **19**, 945 (1976).
Neira, M., and A. C. Payatakes, "Collocation Solution of Creeping Newtonian Flow Through Periodically Constricted Tubes with Piecewise Continuous Wall Profile," *AIChE J.*, **24**, 42 (1978).
Neira, M., and A. C. Payatakes, "Collocation Solution of Creeping Newtonian Flow Through Sinusoidal Tubes," *AIChE J.*, **25**, 725 (1979).
Oh, S. G., and J. C. Slattery, "Interfacial Tension Required for Significant Displacement of Residual Oil," *Soc. Petrol. Eng. J.*, **19** (1979).
Payatakes, A. C., Chi Tien, and R. M. Turian, "A New Model for Granular Porous Media, Part I. Model Formulation," *AIChE J.*, **19**, 58 (1973a).
Payatakes, A. C., Chi Tien, and R. M. Turian, "Part II. Numerical Solution of Steady State Incompressible Newtonian Flow Through Periodically Constricted Tubes," *AIChE J.*, **19**, 67 (1973b).
Payatakes, A. C., Chi Tien, and R. M. Turian, "Further Work on the Flow Through Periodically Constricted Tubes—A Reply," *AIChE J.*, **19**, 1036 (1973c).
Payatakes, A. C., Chi Tien, and R. M. Turian, "Trajectory Calculation of Particle Deposition in Deep Bed Filtration, Part I. Model Formulation," *AIChE J.*, **20**, 889 (1974a).
Payatakes, A. C., Chi Tien, and R. M. Turian, "Part II. Case Study of the Effect of Dimensionless Groups and Comparison with Experimental Data," *AIChE J.*, **20**, 900 (1974b).
Payatakes, A. C., K. M. Ng, and R. W. Flumerfelt, "Oil Ganglion Dynamics During Immiscible Displacement—Model Formulation," *AIChE J.*, **26**, 430 (1980).
Sheffield, R. E., and A. B. Metzner, "Flow of Nonlinear Fluids Through Porous Media," *AIChE J.*, **22**, 736 (1976).
Slattery, J. C., "Interfacial Effects on the Entrapment and Displacement of Residual Oil," *AIChE J.*, **20**, 1145 (1974).
Tien, Chi, and A. C. Payatakes, "Advances in Deep Bed Filtration," *AIChE J.*, **25**, 737 (1979).

Kinetics of the Self-Fouling Oxidation of Hydrogen Sulfide on Activated Carbon

PAN ZHENGLU, HUNG-SHAN WENG, FENG HAN-YU, and J. M. SMITH

Department of Chemical Engineering
University of California
Davis, CA 95616

Most of the prior investigations of the catalytic reaction (on activated carbon)

$$H_2S(g) + \tfrac{1}{2}O_2(g) \rightarrow H_2O(g) + S \qquad (1)$$

have used thermal gravity apparatus, determining the rate from the weight of deposited sulfur. Steijins et al. (1976) reported that the sulfur product deposited on the carbon had some catalytic activity. Coskun and Tollefson (1977) noted that the rate of the reaction decreased with time, presumably due to sulfur deposition. Sreeramamurthy and Menon (1975) found that sulfur powder alone did not show catalytic activity. However, there has not been agreement about the kinetics of the reaction. For example, Cariaso and Walker (1975) concluded that the rate was first order in hydrogen sulfide and zero order in oxygen. Coskun and Tollefson proposed one-half order with respect to hydrogen sulfide, and Steijns et al suggested an oxidation-reduction mechanism. Also quantitative rate equations have not been presented.

Our objectives were first to measure reaction rates on fresh activated carbon, and then to determine the effect of deposited sulfur product. Data were obtained for the fresh catalyst in an isothermal, fixed-bed, differential reactor. The concentration range studied was about 1 to 10% for both hydrogen sulfide and for oxygen; measurements were made at 313 K to 353 K and at 108 kPa. For these conditions no sulfur dioxide is produced; the only products are solid sulfur and water vapor. Most of the deactivation measurements were carried out at 323 K over a time interval of 0 to 780 s. At longer times the rate decreases very slowly. Coskun and Tollefson (1977) found that the only products of the reaction on activated carbon, at temperatures below 473 K, were water and sulfur. Cariaso and Walker (1975) showed that deposited sulfur is not measurably oxidized to sulfur dioxide at temperatures below 413 K. In our chromatographic analyses of the effluent gas we found no other peaks than those for N_2, O_2, H_2S and H_2O. Hence, for our studies with a maximum temperature of 353 K, it was assumed that the only reaction was Eq. 1.

P. Zhenglu is on leave from Tianjin Research Institute of Petrol-Chemical Industry, Tianjin, China; H. Weng, from Cheng Kung University, Tainan, China; and F. Han-Yu, from Gansu Teachers University, Lanzhou, China.

EXPERIMENTAL

The range of flow rates and other operating conditions are summarized in Table 1.

Apparatus

The Pyrex reactor (0.01 m I.D.) is shown with dimensions in Figure 1. The activated-carbon catalyst bed was held in the downflow reactor with a fritted disk. Both the Pyrex reactor and stainless-steel preheater coil (0.0317 m I.D., 2.29 m length) were immersed in a constant temperature bath. Figure 2 is a schematic diagram of the apparatus. Mixtures of oxygen, hydrogen sulfide, and nitrogen were prepared in feed tanks 1 and 2. The temperature was measured with an iron-constantan thermocouple inserted in the middle of the bed. The maximum temperature difference between bath and catalyst bed was 3 K. The catalyst charge was about 1×10^{-4} kg. For runs made with water vapor the gas mixture from the feed tank was passed through a saturator operated at a controlled, constant temperature.

Chemicals

The catalyst was a coal-based activated carbon, type BPL from Pittsburgh Activated Carbon Company. It is a high sulface area, broad pore-size distribution material whose properties are given in Table 2. Granular particles with an average diameter of 0.398×10^{-3} m (32–48 mesh) were used in the catalyst beds. Before use the particles were blown with air to remove fines and degassed with N_2.

TABLE 1. OPERATING CONDITIONS FOR FRESH CATALYST RUNS

Temperature	313 to 353 K
Pressure	108.1 kPa
H_2S Concentration (Avg.)[a]	0.41 to 4.35×10^{-3} kmol/m^3
O_2 Concentration (Avg.)[a]	0.11 to 4.07×10^{-3} kmol/m^3
H_2O Concentration (Feed)[a]	0 to 0.5×10^{-3} kmol/m^3
Conversion Range of H_2S	0.03 to 0.26
Flow Rate of Feed Gas[a]	2.5×10^{-6} m^3/s (at 298 K, 101.3 kPa)

[a] Measured at 298 K and 101.3 kPa.